

# A Novel BMP2-Coprecipitated, Layer-by-Layer Assembled Biomimetic Calcium Phosphate Particle: A Biodegradable and Highly Efficient Osteoinducer

Yuanna Zheng, DDS, PhD;<sup>1\*†</sup> Gang Wu, DDS, MD, PhD;<sup>1\*</sup> Tie Liu, DDS, MS;<sup>\*</sup> Yi Liu, DDS;<sup>†</sup> Daniel Wismeijer, DDS, PhD;<sup>\*</sup> Yuelian Liu, DDS, PhD<sup>\*</sup>

---

---

## ABSTRACT

*Purpose:* To repair large-size bone defects, most bone-defect-filling materials in clinic need to obtain osteoinductivity either by mixing them with particulate autologous bone or adsorbing bone morphogenetic protein 2 (BMP2). However, both approaches encounter various limitations. In this study, we hypothesized that our novel particles of biomimetic BMP2-coprecipitated calcium phosphate (BMP2-cop.BioCaP) could serve as an independent and biodegradable osteoinducer to induce bone formation efficiently for these bone-defect-filling materials, for example, deproteinized bovine bone (DBB).

*Materials and Methods:* We alternately layer-by-layer assembled amorphous and crystalline CaP triply to enable a “bamboo-like” growth of the particles. We functionalized BioCaP by coprecipitating BMP2 into the most outer layer of BioCaP. We monitored the degradation, osteoinductivity, and foreign-body reaction of either BMP2-cop.BioCaP or its combination with DBB in an ectopic site in rats.

*Results:* After 5 weeks, the BMP2-cop.BioCaP significantly induced new bone formation not only alone but also when mixed with DBB. Its osteoinductive efficiency was 10-fold higher than the adsorbed BMP2. Furthermore, BMP2-cop.BioCaP also reduced significantly the host foreign-body reaction to DBB in comparison with the adsorbed BMP2. After a 5-week implantation, more than 90% of BMP2-cop.BioCaP degraded.

*Conclusions:* These findings indicate a promising clinical potential for BMP2-cop.BioCaP in the repair of large-size bone defects.

**KEY WORDS:** biomimetic, bone morphogenetic protein, bone regeneration, calcium phosphate, layer-by-layer, osteoinducer

---

---

\*Department of Oral Implantology and Prosthetic Dentistry, Academic Centre for Dentistry Amsterdam (ACTA), Research Institute MOVE, VU University and University of Amsterdam, Amsterdam, The Netherlands; <sup>†</sup>School of Stomatology/Dental Clinic, Zhejiang Chinese Medical University, Hangzhou, China

Reprint requests: Dr. Yuelian Liu, Department of Oral Implantology and Prosthetic Dentistry, Academic Centre for Dentistry Amsterdam (ACTA), Research Institute MOVE, VU University and University of Amsterdam, Gustav Mahlerlaan 3004, 1018 LA Amsterdam, The Netherlands; e-mail: y.liu@acta.nl

<sup>†</sup>Yuanna Zheng and Gang Wu contributed equally.

© 2013 Wiley Periodicals, Inc.

DOI 10.1111/cid.12050

## INTRODUCTION

Large-size bone defects exceed the self-healing capacity of bone tissue and often a profibrotic microenvironment is formed in the defects.<sup>1</sup> To realize their osseous restoration, bone-defect-filling materials are indispensable. Although autografts are still regarded as the “gold standard” bone-defect-filling materials, their application is still limited because of the low available quantity as well as donor-site pain and morbidity.<sup>2</sup> Consequently, allografted, xenografted, and synthetic calcium phosphate (CaP)-based materials (e.g., deproteinized bone and biphasic CaP) are widely adopted clinically for the treatment of large-size bone defects. These materials are

also highly osteoconductive so that they can significantly enhance the migration of osteogenic cells. However, such an enhancement is still too limited to realize osseous restoration. They intrinsically lack osteoinductivity for inducing bone regeneration in a profibrotic environment. One common approach used clinically is to combine bone-defect-filling materials with ground autografts<sup>3</sup> — which supplies the necessary osteogenic elements — for repairing large-size bone defects. In this case, the above-mentioned limitations of autografts ensue.

One promising approach to this problem is to confer osteoinductivity to these CaP-based materials by using an osteoinductive agent, such as bone morphogenetic protein 2 (BMP2). BMP2 is a dimeric disulfide-linked polypeptide growth factor under transforming growth factors- $\beta$  superfamily. BMP2 has been approved by Food and Drug Administration (FDA) and shown to induce bone formation in animal studies and clinical trials.<sup>4-7</sup> A consensus has been reached that the *in vivo* osteoinductive efficiency of BMP2 is highly dependent on its release kinetics. The present mode of delivery in clinic — superficial adsorption of BMP2 onto bone-defect-filling materials<sup>8</sup> — is associated with a rapid and burst release.<sup>9,10</sup> Most of such delivered BMP2 is released too rapidly to induce a sustained osteogenic activity at the site of the implantation. This difficulty cannot be overcome satisfactorily merely by increasing the loading dose of BMP2. Apart from the tremendous expense that would be incurred, the transient high local concentration of BMP2, which would be generated, could induce various side effects, such as an excessive stimulation of local bone resorption and the induction of bone formation at unintended sites.<sup>11-13</sup>

To be optimally osteoinductive, BMP2 needs to be delivered to target sites at low concentrations in a sustained manner. One such approach is to coprecipitate BMP2 into a thin layer of biomimetic CaP (BioCaP) coating that is prepared on the surfaces of biomaterials.<sup>4</sup> We have recently shown that coating-coprecipitated BMP2 induced a significantly higher volume of new bone surrounding the biomaterials than the superficially adsorbed BMP2.<sup>14</sup> In addition, the coating-coprecipitated BMP2 could also suppress significantly the host foreign-body reaction to the biomaterials, while the superficially adsorbed BMP2 could not.<sup>15</sup> On the other hand, although the biomimetic coating technique is broadly applicable to a series of bone-defect-filling materials,<sup>16</sup> its application is not unlimited because of the

dependence of coating growth on the physicochemical properties of the underlying biomaterials as well as the need to prepare the coatings on these materials.

Recently, we made a breakthrough in modifying the biomimetic coating procedure. Thereby, we have for the first time alternately layer-by-layer assembled BMP2-coprecipitated BioCaP (BMP2-cop.BioCaP) particles that could serve as an independent “osteoiducer.” This novel BMP2-cop.BioCaP was designed to be mixed directly with clinically used bone-defect-filling materials to induce bone formation. In this study, we monitored the biological properties of BMP2-cop.BioCaP such as degradation, osteoinductivity, and foreign-body reaction. We also ascertained whether BMP2-cop.BioCaP could efficiently induce bone formation surrounding, and suppress the host foreign-body reaction to a clinically used bone-defect-filling material — deproteinized bovine bone (DBB).

## MATERIALS AND METHODS

### *In Vitro* Investigation

*Preparation of Layer-by-Layer Assembled BioCaP Particles with or without Coprecipitated BMP2.* The protocol (Figure 1) to produce the layer-by-layer assembled BioCaP particles was derived from our well-established biphasic biomimetic coating protocols.<sup>4,17,18</sup> Briefly, microparticles of amorphous CaP were obtained in 2,000 mL of the fivefold-concentrated simulated body fluid (684 mM NaCl; 12.5 mM CaCl<sub>2</sub>·2H<sub>2</sub>O; 21 mM NaHCO<sub>3</sub>; 5 mM Na<sub>2</sub>HPO<sub>4</sub>·2H<sub>2</sub>O; and 7.5 mM MgCl<sub>2</sub>·2H<sub>2</sub>O [Sigma, St. Louis, MO, USA]) for 24 hours at 37°C. Thereafter, the amorphous CaP microparticles were immersed in 1,000 mL of a supersaturated CaP solution (40 mM HCl; 2 mM Na<sub>2</sub>HPO<sub>4</sub>·2H<sub>2</sub>O; 4 mM CaCl<sub>2</sub>·2H<sub>2</sub>O; and 50 mM TRIS base [Sigma] [pH 7.4]) for 48 hours at 37°C. Thereby, a thick layer of crystalline CaP was deposited on amorphous CaP microparticles. After drying at room temperature, these particles were then immersed in the fivefold simulated body fluid (24 hours) and the supersaturated CaP solution (48 hours) alternately for a total of three cycles. During the preparation of the final crystalline CaP layer, BMP2 (INFUSE® Bone Graft, Medtronic, Minneapolis, MN, USA) was introduced into this supersaturated CaP solution at a final concentration of 2  $\mu$ g/mL and coprecipitated with the crystalline CaP layer. The samples were then freeze dried. The entire procedure was conducted under sterile conditions.

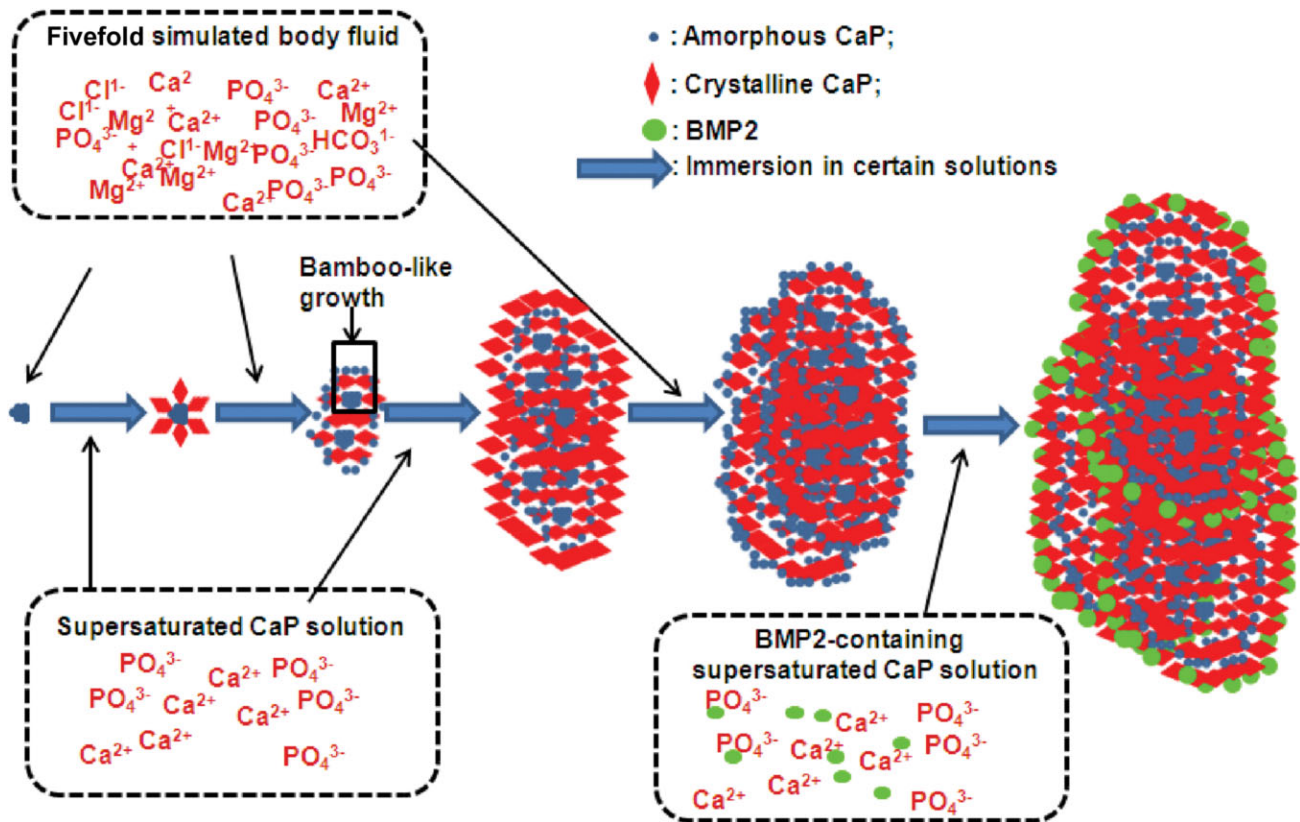


**Figure 1** Schematic graphs demonstrating the layer-by-layer assembling process of biomimetic calcium phosphate (BioCaP). Microparticles of amorphous CaP that were initially obtained from the fivefold simulated body fluid were immersed into supersaturated CaP solution for 48 hours and the fivefold simulated body fluid for 24 hours alternately. Thereby, amorphous CaP and crystalline CaP were layer-by-layer assembled. Then, the particles were immersed into a supersaturated CaP solution with 2  $\mu\text{g}/\text{mL}$  bone morphogenetic protein 2 (BMP2). After 48 hours, the particles were air dried and ready for use. The increase of particle size was attributed to both the layer-by-layer growth of coatings and the aggregation of particles by the growing coatings.

*Surface Characterization of the BioCaP.* The surface characteristics of BioCaP were evaluated in a scanning electron microscope (XL 30, Philips, Eindhoven, the Netherlands). For this purpose, samples of the material were mounted on aluminum stubs and sputtered with gold particles to a thickness of 10 to 15 nm.

*Determination of the Amount of the Coprecipitated BMP2.* The amount of coprecipitated BMP2 was determined using a commercially available enzyme-linked immunosorbent assay (ELISA) kit (PeproTech, London, UK). 0.05 g of BMP2-cop.BioCaP was dissolved in 1 mL 0.5 M Ethylenediaminetetraacetic acid (EDTA) (pH 8.0). The ELISA was performed according to the manufacturer's instructions. Three samples were used for this purpose.

*Confirmation of the Homogeneous Distribution of the Coprecipitated Protein by Fluorescence Microscopy.* To investigate the distribution of the coprecipitated

protein within BioCaP, BMP2 was substituted by a model protein – bovine serum albumin that had been conjugated with fluorescein isothiocyanate<sup>19</sup> (FITC-BSA [Sigma]). FITC-BSA was introduced into the supersaturated CaP solution at a final concentration of 2  $\mu\text{g}/\text{mL}$ . After freeze drying, the coated samples were embedded in methyl methacrylate. Six hundred-micrometer-thick sections were prepared and affixed to Plexiglas holders. These sections were then ground down to a thickness of 80  $\mu\text{m}$  for an inspection in a fluorescence microscope.

*In Vitro Monitoring of the Release Kinetics of the Coprecipitated Protein in BioCaP.* To monitor the release kinetics of the coprecipitated protein in BioCaP, FITC-BSA (2  $\mu\text{g}/\text{mL}$ ) was introduced into supersaturated CaP solution for the final immersion. Six samples were used to determine the total amount of coprecipitated FITC-BSA. These samples were immersed in 1 mL of 0.5% EDTA (pH 8.0) and vortexed twice for 5 minutes to

ensure complete dissolution of coatings. The supernatants were withdrawn for analysis of total loading of FITC-BSA.

To monitor the release kinetics, six samples of DBB mixed with FITC-BSA-cop.BioCaP at a volume ratio of 4:1 and six samples of DBB bearing an equivalent amount of adsorbed FITC-BSA (included for the purpose of comparison and prepared likewise as the adsorption of BMP2) were incubated in sealed 10-mL glass tubes containing 2 mL of phosphate-buffered 0.9% saline (pH 7.4). The tubes were incubated for up to 35 days in a shaking water bath (60 agitations/min), which was maintained at 37°C. The sampling and measurement with spectrophotometer were performed following the protocol as previously published.<sup>15</sup> Fluorescence readings were converted to amounts of protein using a standard curve, which was generated by preparing a dilution series of FITC-BSA in 5 mL of phosphate-buffered 0.9% saline. The temporal release of FITC-BSA was expressed as a percentage of the total amount that had been coprecipitated into the crystalline layer of the BioCaP or that had been adsorbed directly onto the DBB particles.

### In Vivo Investigation

We adopted a subcutaneous bone induction model in rats to further evaluate the BMP2-cop.BioCaP in vivo in aspects of degradation, osteoinductivity, and foreign-body reactivity. We measured the following parameters: (1) volume density of newly formed bone; (2) volume density of foreign-body giant cells (FBGCs); (3) volume density of BioCaP; and (4) osteoinductive efficiency of BMP2.

*Grouping.* As an experimental animal model, we used adult male Wistar rats (200–220 g). Six groups were established ( $n = 6$  animals per group): (1) BioCaP; (2) BMP2-cop.BioCaP; (3) DBB alone; (4) DBB bearing adsorbed BMP2; (5) DBB mixed with  $0.07 \text{ cm}^3$  BioCaP; and (6) DBB mixed with  $0.07 \text{ cm}^3$  BMP2-cop.BioCaP. The amount of BMP2-cop.BioCaP (0.07) was determined according to our previous study.<sup>15</sup> It showed that about 10 to 15  $\mu\text{g}$  of the coating-coprecipitated BMP2 could sufficiently induce bone formation. About  $0.07 \text{ cm}^3$  BMP2-cop.BioCaP contains  $10.29 \pm 1.94 \mu\text{g}$  BMP2 according to the ELISA result.

0.15 g of DBB (about  $0.35 \text{ cm}^3$ ) per sample was used. The samples of DBB bearing adsorbed BMP2

(about 13.5  $\mu\text{g}$ ) were prepared as described previously.<sup>15</sup> The loading process was achieved by introducing a 75  $\mu\text{L}$  aliquot of stock solution (0.18  $\mu\text{g}/\mu\text{L}$ ) into 1-mL Eppendorf tubes containing 0.15 g of DBB particles.

*Surgery and Histology.* Animal experiments were conducted with the permission of and in accordance with the regulations laid down by the Animal Protection Commission of the State of Bern (Switzerland). Eighteen rats were used in this study. Each rat received two samples from two different groups: they are either non-BMP2-containing discs (groups 1, 3, and 5) or BMP2-containing discs (groups 2, 4, and 6). To the end, six animals were used for each group ( $n = 6$  animals per group).

The rats were acclimatized to their new surroundings for 5 days. Housing is in compliance with the national guidelines for animal experimentation. Surgery was performed under conditions of general anesthesia (using Vetalar® [ketamine hydrochloride], Boehringer Ingelheim Vetmedica, Inc., St. Joseph, MO, USA).<sup>4</sup> Two samples per rat were surgically implanted within lateral dorsal subcutaneous pockets (one on the left side and one on the right) and were trapped therein by suturing the incision site. After surgery, the rats were kept in cages of animal facility of Bern University for 1, 2, and 3 weeks. The animals were fed ad libitum with hay, granulated food, and water.

Five weeks after surgery, the samples were retrieved, chemically fixed, and embedded in methyl methacrylate as previously reported.<sup>4,18</sup> By applying a systematic random-sampling strategy,<sup>20</sup> the samples were sawed vertically to the short axis, into 10 to 12 slices of 600  $\mu\text{m}$  thickness with 1 mm apart. Odd- or even-numbered slices of each sample were separately mounted on Plexiglas holders and polished. The odd-numbered slices were surface stained with McNeal's tetrachrome, basic fuchsin, and toluidine blue O<sup>21</sup> for the histomorphometric analysis of various parameters (see below). The even-numbered slices were subjected to the tartrate-resistant acid phosphatase (TRAP) reaction<sup>4,22</sup> and counterstained with methyl green. They were used to estimate the volume density of multinucleated osteoclasts. Applying a two-step systematic random-sampling strategy, 25 to 30 images at a final magnification of  $\times 320$  were recorded in a Leica DMRA microscope (Leica, Wetzlar, Germany) and printed in color for the histomorphometric analysis.

*Histomorphometric Analysis.* In the present study, the space under the fibrous capsule that embraced the whole block of implants (subcapsular space) was taken as the reference space. The reference space was estimated using Cavalieri's methodology.<sup>23</sup> This involves measuring the cross-sectional area of a defined number of tissue sections at a fixed distance apart through the reference volume. The cross-sectional area of each section was estimated using the point-counting technique.<sup>24</sup>

The volume densities of the bone, the multinucleated cells, and the remaining materials were determined stereologically from its area density on tissue sections by the point-counting technique.<sup>24</sup> The volume density of FBGCs was obtained by subtracting that of TRAP-positive osteoclasts from that of multinucleated cells.<sup>4</sup> To compare the foreign-body reaction with either BMP2-cop.BioCaP, BioCaP, or DBB in different groups, the volume density of FBGCs was normalized to the corresponding volume density of BMP2-cop.BioCaP, BioCaP, or DBB.

The total volume of bone and the remaining BioCaP material were estimated by multiplying the volume densities of each parameter by the corresponding subcapsular reference volume. The osteoinductive efficiency of BMP2 was estimated by dividing the total volume of bone by the amount of BMP2. Because more than 90% of BMP2-cop.BioCaP was degraded, we assumed that all the coprecipitated BMP2 in its outer layer was completely used. The BMP2 that was adsorbed onto DBB should also be exhausted after 5 weeks because it exhibited a burst release. Therefore, we use the total loading of BMP2 to estimate the osteoinductive efficiency.

## Statistical Analysis

All data are presented as mean values together with the standard deviation (mean  $\pm$  standard deviation). Data were compared using a one-way analysis of variance with the significance level being set at  $p < .05$ . Post hoc comparisons were made using Bonferroni's corrections.

## RESULTS

### In Vitro Characterization

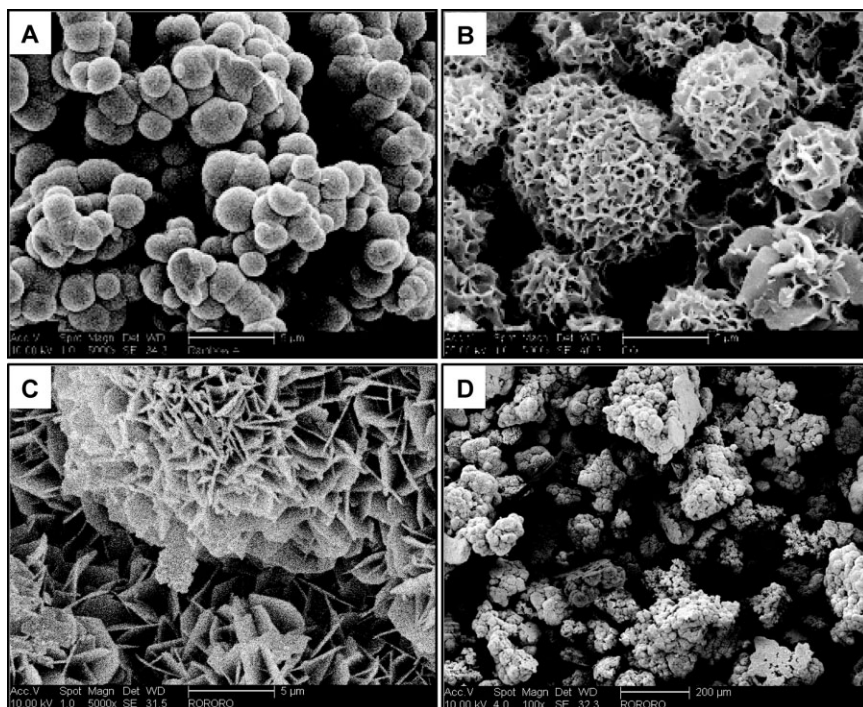
In this study, we assembled three-dimensional particles using this novel biomimetic layer-by-layer assembling technique. Under scanning electron microscopy, the amorphous CaP microparticles that were derived from

the fivefold simulated body fluid in the first cycle showed morphology of irregular clusters of microspheres with a diameter of 1.5 to 3  $\mu\text{m}$  (Figure 2A). After immersing these amorphous CaP microparticles in supersaturated CaP solution for 48 hours, a crystalline CaP deposited on their surfaces and showed plate or needle-like crystals (see Figure 2B). After three cycles of alternate immersion, the particle size increased from the initial 5 to 20  $\mu\text{m}$  up to 100 to 1000  $\mu\text{m}$  (see Figure 2D) with a crystalline outer layer (see Figure 2C). The coprecipitated protein is located within the whole outer crystalline CaP layer (Figure 3A). As anticipated, the FITC-BSA that was adsorbed onto DBB was released rapidly, being completely exhausted after 13 days (see Figure 3B). In contrast, protein that was coprecipitated into BioCaP was released gradually and at a steady rate after the third day until the 35th day, at which in juncture the initial depot had been depleted by no more than 50.1% (see Figure 3B). The total loading of BMP2 in 0.35  $\text{cm}^3$  BMP2-cop.BioCaP is  $51.13 \pm 9.68 \mu\text{g}$ , with a coprecipitation rate of  $30.1 \pm 5.7\%$ .

### In Vivo Study

*Histological Results.* Five weeks after the subcutaneous implantation, BioCaP distributed compactly and did not induce new bone formation (Figure 4A). Connective tissue infiltrated into the BioCaP particles, on the surfaces of which multinucleated FBGC was frequently found (see Figure 4A1). In contrast, BMP2-cop.BioCaP distributed loosely and induced a large volume of new bone (see Figure 4B). BMP2-cop.BioCaP was tightly integrated into the new bone (see Figure 4B1).

Five weeks after implantation, new bone was only found surrounding the DBB either with adsorbed BMP2 (Figure 5B) or mixed with BMP2-cop.BioCaP (see Figure 5D). No new bone formation was found surrounding the DBB either alone (see Figure 5A) or mixed with BioCaP (see Figure 5C). Bone was deposited abundantly surrounding the DBB with BMP2-cop.BioCaP (see Figure 5D), but only sporadically surrounding the DBB with adsorbed BMP2 (see Figure 5B). The remaining BioCaP showed clusters of round, ellipse, or irregular microparticles (see Figure 5C1). They distributed among the DBB particles (see Figure 5C) with connective tissue filling in between (see Figure 5C1). For the DBB with BMP2-cop.BioCaP, bone tissue formed with BMP2-cop.BioCaP as center and deposited on the surfaces of both BMP2-cop.BioCaP and DBB (see



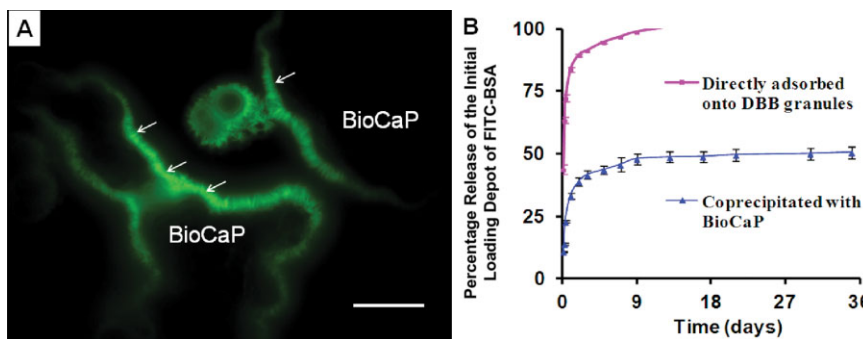
**Figure 2** Scanning electron micrographs depicting the morphologies of the initial amorphous calcium phosphate (CaP) particles (A), the initial layer of crystalline CaP (B), and the final bone morphogenetic protein 2-coprecipitated biomimetic CaP (C and D). Bars = 5 μm in A, B, and C. Bar = 200 μm in D.

Figure 5D). Bone tissue was found tightly integrated with BMP2-cop.BioCaP and DBB without intervening tissues (see Figure 5D1).

**Histomorphometric Results.** The volume density of bone surrounding BMP2-cop.BioCaP was  $0.36 \pm 0.07 \text{ mm}^3/\text{mm}^3$  (Figure 6A). The remaining percentage of BMP2-cop.BioCaP ( $5.6 \pm 2.1\%$ ) was significantly lower than that of BioCaP ( $34.2 \pm 6.4\%$ ) (see Figure 6B). The volume ratio of FBGCs to BMP2-cop.BioCaP

( $0.063 \pm 0.0198 \text{ mm}^3/\text{mm}^3$ ) was also significantly lower than that to BioCaP ( $0.110 \pm 0.0188 \text{ mm}^3/\text{mm}^3$ ) (see Figure 6C).

The volume density of bone surrounding DBB mixed with BMP2-cop.BioCaP ( $0.06 \pm 0.03 \text{ mm}^3/\text{mm}^3$ ) was significantly higher than that surrounding DBB with adsorbed BMP2 ( $0.007 \pm 0.009 \text{ mm}^3/\text{mm}^3$ ) (Figure 7A). The osteoinductive efficiency of BMP2 in the group of DBB mixed with BMP2-cop.BioCaP was 10-fold higher than that in the group of DBB with



**Figure 3** (A) Fluorescence micrographs depicting the distribution of coprecipitated protein in the outer layer of biomimetic calcium phosphate (BioCaP). Fluorescein isothiocyanate-bovine serum albumin (FITC-BSA) (green signal) was used to as a substitute for bone morphogenetic protein 2 (BMP2). Bar = 100 μm. (B) Graph depicting the in vitro release kinetics of FITC-BSA from deproteinized bovine bone (DBB) with BMP2-cop.BioCaP and DBB with adsorbed FITC-BSA.

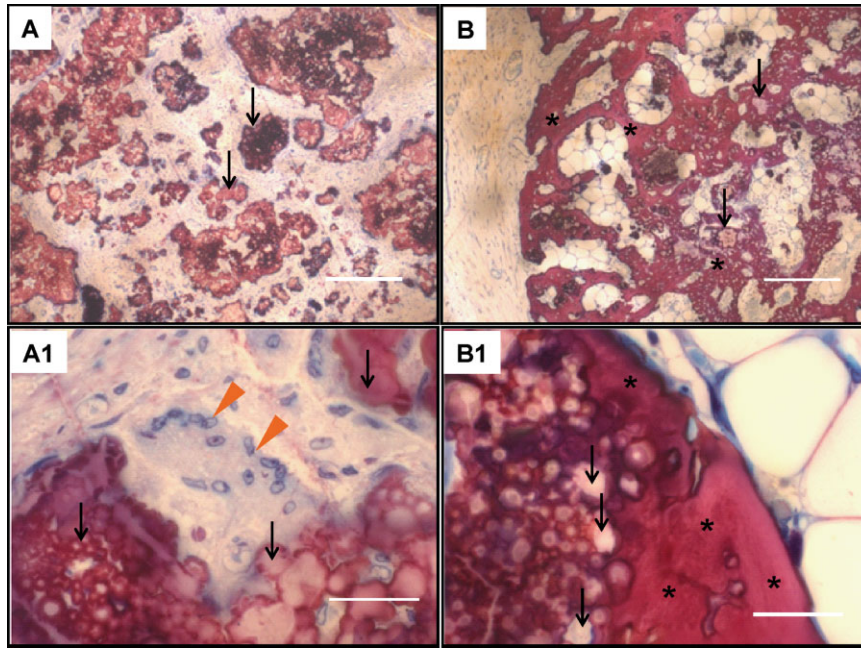


**Figure 4** Light micrographs of the cross sections through biomimetic calcium phosphate (BioCaP) (A and A1) and bone morphogenetic protein 2-coprecipitated BioCaP (B and B1) after a 5-week implantation in subcutaneous site in rats. The sections were stained with McNeal's tetrachrome, basic fuchsin, and toluidine blue O. Yellow arrows point to the foreign-body giant cells lying on BioCaP. Black arrows point to the remaining BioCaP. Asterisks indicate the newly formed bone. Bars = 200  $\mu\text{m}$  in A and B. Bars = 30  $\mu\text{m}$  in A1 and B1.

adsorbed BMP2 (see Figure 7B). The remaining percentage of BioCaP in the group of DBB with BMP2-cop.BioCaP ( $8.4 \pm 5.5\%$ ) was significantly lower than that in the group of DBB with BioCaP ( $24.9 \pm 6.1\%$ ) (see Figure 6B). The mixture with DBB did not significantly influence the remaining percentage of BioCaP regardless of the coprecipitation of BMP2 (see Figure 6). The volume ratio of FBGCs to BMP2-cop.BioCaP ( $0.013 \pm 0.018 \text{ mm}^3/\text{mm}^3$ ) was also significantly lower than that to BioCaP ( $0.155 \pm 0.019 \text{ mm}^3/\text{mm}^3$ ) at the presence of DBB (see Figure 6C). The volume ratio of FBGCs to the DBB mixed with BMP2-cop.BioCaP ( $0.009 \pm 0.005 \text{ mm}^3/\text{mm}^3$ ) was significantly lower than that to the DBB either alone ( $0.039 \pm 0.012 \text{ mm}^3/\text{mm}^3$ ), with adsorbed BMP2 ( $0.038 \pm 0.006 \text{ mm}^3/\text{mm}^3$ ), or with BioCaP ( $0.043 \pm 0.004 \text{ mm}^3/\text{mm}^3$ ) (see Figure 7C).

## DISCUSSION

In this study, we have, for the first time, developed three-dimensional BioCaP particles (100–1000  $\mu\text{m}$ ) by modifying the principle for preparing the thin (10–50  $\mu\text{m}$ ) and substrate-dependent BioCaP coatings. In this novel particles, the advantage of the coatings in coprecipitating and slowly releasing proteinaceous cytokines was maintained. We showed that this novel BMP2-

cop.BioCaP, serving as an independent “osteoinducer,” could induce bone formation efficiently and suppress the host foreign-body reaction when it was mixed with DBB – a clinically used bone-defect-filling material. In addition, BMP2-cop.BioCaP also exhibited a proper degradation rate in vivo.

In our previous studies, we have already shown that the BMP2-coprecipitated biomimetic coating is very broadly applicable to bone-defect-filling materials and dental implants. This was proven by the success in the preparation of this coating on a broad range of biomaterials (e.g., metallic,<sup>4,25</sup> inorganic,<sup>15</sup> and polymeric materials<sup>26</sup>) that have completely different geometries, topographies, and surface chemistries.<sup>16</sup> Albeit so, this type of biomimetic coating on bone-defect-filling materials has the limitation that their growth relies still highly on the proper surface roughness and/or active surface chemistry of the bone-defect-filling materials.<sup>16</sup> In this study, we modified the biomimetic coating technique and developed this BMP2-cop.BioCaP with an aim of completely breaking through these limitations. The BMP2-cop.BioCaP exhibited no dependence on the physiochemical properties of bone-defect-filling materials and thus can possibly be applied with any kind of granular bone-defect-filling materials used clinically.

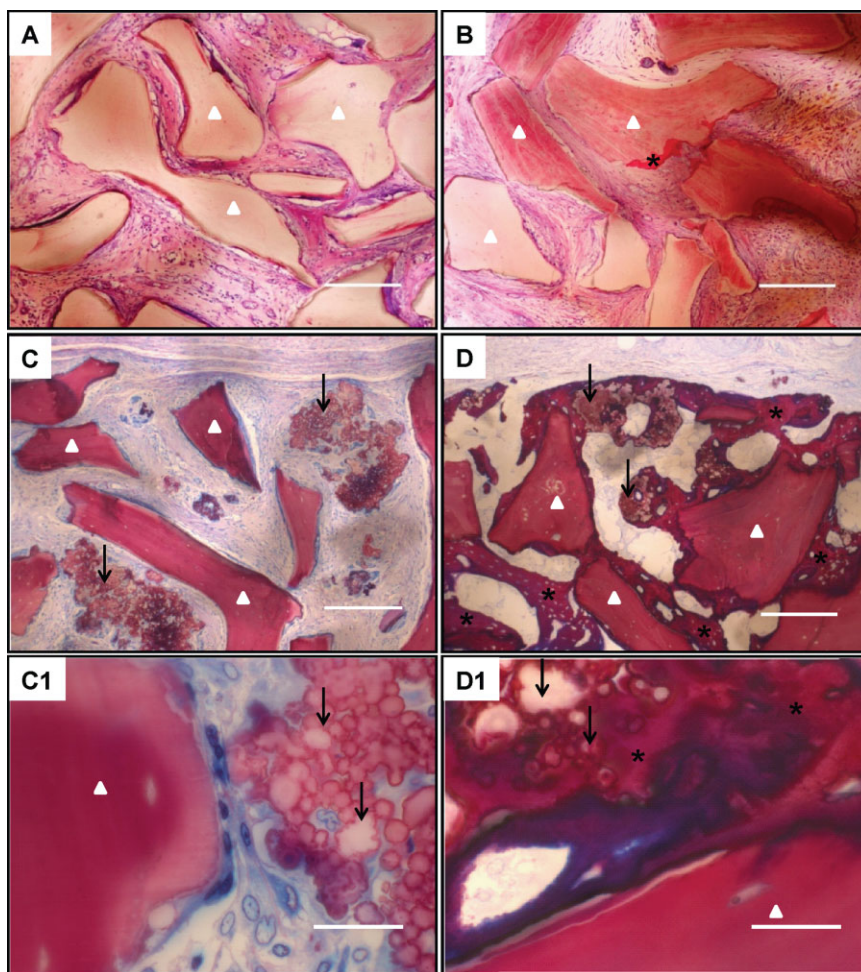


**Figure 5** Light micrographs of the cross sections through deproteinized bovine bone (DBB) alone (A), DBB with adsorbed bone morphogenetic protein 2 (BMP2) (B), DBB with biomimetic calcium phosphate (BioCaP) (C and C1), and DBB with BMP2-cop.BioCaP (D and D1) after a 5-week implantation in subcutaneous site in rats. The sections were stained with McNeal's tetrachrome, basic fuchsin, and toluidine blue O. Asterisks indicate the newly formed bone. Bars = 200  $\mu\text{m}$  in A, B, C, and D. Bars = 30  $\mu\text{m}$  in C1 and D1.

Meanwhile, this BMP2-cop.BioCaP is also easily handled clinically, which will significantly favor its clinical application.

The alternate assembling of the amorphous and crystalline layer was indispensable to increase significantly the volume of BioCaP particles. This is because the amorphous CaP layer is very thin (1.5–10  $\mu\text{m}$ ) and the crystalline CaP is hardly beyond 100  $\mu\text{m}$ . By this alternate layer-by-layer approach, we use the amorphous CaP layer as a connection and seeding layer for the growth of another layer of crystalline CaP. The BioCaP grows in a “bamboo-like” pattern with the amorphous CaP as the nodes and the crystalline CaP as the internodes. After three cycles of alternate soaking in the fivefold simulated body fluid and supersaturated CaP solution alternately (Figure 1), the size of the BioCaP

significantly increased from the initial 5 to 20  $\mu\text{m}$  to 100  $\mu\text{m}$  to 1 mm (Figure 2). The increase in size was attributed both to the “bamboo-like” layer-by-layer growth of coatings and to the aggregation of underlying particles by the growing coatings (Figure 1). The current size of BMP2-cop.BioCaP seemed correct for sustaining the osteoinductive effect of coprecipitated BMP2 because a large amount of new bone was induced with high efficiency (Figure 7B).

Besides the size, the degradability of a CaP-based biomaterial is very important for the in vivo longevity and efficacy of its biological effects.<sup>27</sup> After 5 weeks, 60 to 82% of BioCaP degraded (Figure 6B), which indicated a significantly higher degradability of BioCaP than most of the clinically used CaP-based bone-filling materials. Such a rapid degradation is associated with its high

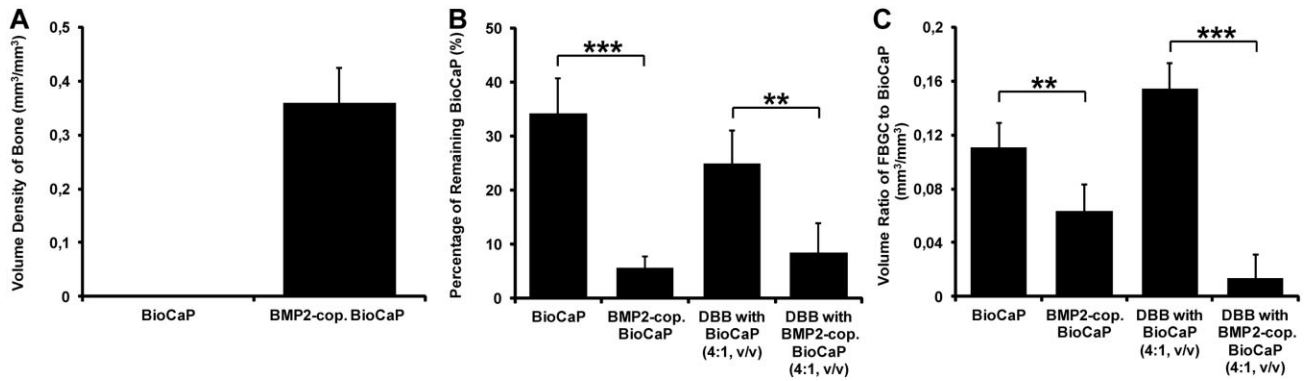


**Figure 6** Graph depicting the volume density of new bone (A), percentage of remaining bone morphogenetic protein 2 (BioCaP) (B), and volume ratio of foreign-body giant cells (FBGCs) to BioCaP (C) that were associated with BioCaP within the subcapsular space (reference volume) for the four groups, 5 weeks after subcutaneous implantation in rats. Mean values ( $n = 6$  animals per group) are represented together with the standard deviation.  $*p < .05$ ;  $**p < .01$ ;  $***p < .001$ . BMP2-cop.BioCaP = bone morphogenetic protein 2-coprecipitated BioCaP; DBB = deproteinized bovine bone.

dissolubility of BioCaP. This is because BioCaP was prepared in biomimetic principle without the involvement of nonphysiological conditions (e.g., high temperature) and was composed of both amorphous CaP and crystalline calcium-deficient hydroxyapatite with a low crystallinity.<sup>26</sup> In contrast, most of the clinically used bone-defect-filling materials are sintered, which leads to the significantly increased crystallinity and thus decreased dissolubility.<sup>28</sup>

Apart from the spontaneous dissolution, the degradation of a material is also accelerated by many types of cells (e.g., fibroblasts and monocytes/macrophages) through phagocytotic mechanisms.<sup>29</sup> When their phagocytic capacity is exceeded, macrophages can also fuse to form FBGCs. In contrast, these multinucleated FBGCs had a significantly higher resorptive efficiency<sup>30</sup> and

played a major role in the degradation of BioCaP. Interestingly, although the volume ratio of FBGCs to BMP2-cop.BioCaP was significantly decreased (Figure 6C), the degradation rate of BMP2-cop.BioCaP was significantly increased in comparison with BioCaP (Figure 6B). In fact, the suppression of FBGCs to CaP coatings in the presence of coprecipitated BMP2 could be found from 2 to 3 weeks.<sup>4</sup> These findings suggested that other resorption mechanisms played key roles in the degradation of BMP2-cop.BioCaP. The activities of osteoblasts and osteoclasts during the osteogenesis may account for this phenomenon. Besides, except phagocytic activity,<sup>29</sup> osteoblasts-mediated mineralization can generate many protons<sup>31</sup> that may promote the degradation of BMP2-cop.BioCaP. Conventionally, these protons have to be neutralized by an extracellular buffering system to

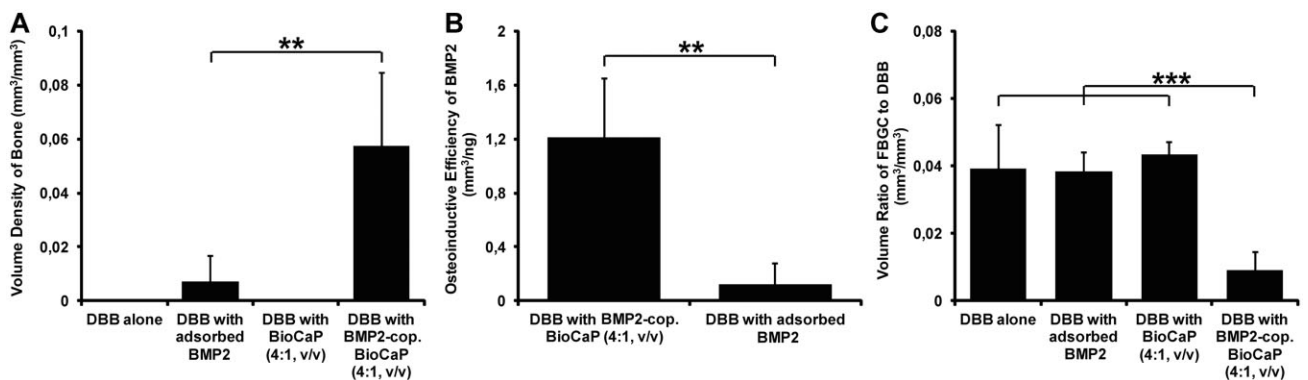


**Figure 7** Graph depicting the volume density of new bone (A), osteoinductive efficiency of bone morphogenetic protein 2 (BMP2) (B), and volume ratio of foreign-body giant cells (FBGCs) to bone morphogenetic protein 2 (BioCaP) (C) that were associated with BioCaP within the subcapsular space (reference volume) for the four groups, 5 weeks after subcutaneous implantation in rats. Mean values ( $n = 6$  animals per group) are represented together with the standard deviation.  $*p < .05$ ;  $**p < .01$ ;  $***p < .001$ . DBB = deproteinized bovine bone.

prevent their accumulation.<sup>32</sup> CaP materials with a high dissolubility may directly neutralize the protons, which promote the activities of osteoblasts. The calcium and phosphate ions generated in this way can greatly support the process of osteogenesis. Consequently, a CaP material that bears the greater solubility shows the higher osteoconductivity.<sup>33</sup> In this study, the osteogenesis was significantly promoted by the coprecipitated BMP2, which also increased significantly the osteoblast-mediated degradation and reuse of BioCaP. On the other hand, the mixture with DBB did not significantly influence the degradation rate of either BioCaP or BMP2-cop.BioCaP (Figure 6B), which indicated that the degradation property of BMP2-cop.BioCaP was not influenced by the targeting bone-defect-filling materials.

The release kinetics is a crucial factor for the osteoinductive efficiency of BMP2. In a clinical application, BMP2 is simply adsorbed superficially onto the bone-defect-filling materials, which is associated with a high-dose burst release and thus low osteoinductive efficiency.<sup>8</sup> In contrast, the coating-coprecipitated BMP2 showed a slow and sustained release and thus a significantly higher osteoinductive efficiency than the adsorbed BMP2.<sup>14,15</sup> In line with this principle, DBB with BMP2-cop.BioCaP induced significantly higher volume density of bone than the DBB with adsorbed BMP2 (Figure 7A). Accordingly, the osteoinductive efficiency of BMP2 in the group of DBB with BMP2-cop.BioCaP was 10-fold higher than that in the group of DBB with adsorbed BMP2 (Figure 7B). These findings indicated that BMP2-cop.BioCaP could act as a powerful “osteoiducer” to induce efficiently new bone formation for other granular clinically used bone-defect-filling materials. Although the newly formed bone originated from the BMP2-cop.BioCaP, it did not stay unattached but integrated tightly onto the DBB (Figure 5D1) without the intervening of connective tissues. Thereby, DBB, BMP2-cop.BioCaP, and the new bone form an interconnected bony network (Figure 5D). In contrast, for the BioCaP without the coprecipitation of BMP2, BioCaP and DBB were isolated by fibrous connective tissues (Figure 5C1) and no bone tissue was detected (Figure 5C).

One concern associated with the use of DBB is its biocompatibility. Although DBB can integrate with bone in a pro-osteogenic environment such as in noncritical-sized bone defects and/or in the presence of a sufficiency of autologous bone chips,<sup>34</sup> it can provoke significant foreign-body reactions in a profibrotic environment

such as at a subcutaneous site<sup>35</sup> or in critical-sized bony defects.<sup>1</sup> Foreign-body reactivity is histologically characterized by the local accumulation of macrophages, their fusion to form FBGCs, and the deposition of dense fibrous connective tissue.<sup>30</sup> FBGCs begin to appear between the 2nd and the 10th days after implantation.<sup>36</sup> They often persist for the whole lifetime of the implant<sup>37</sup> and their presence is known to be associated with the failure of biomaterials.<sup>30</sup> The foreign-body reaction may significantly hinder the regeneration of bone and the osseointegration of DBB. In this study, we found that the volume ratio of FBGCs to DBB was significantly lower in the group of DBB with BMP2-cop.BioCaP than that in the group of either DBB alone, DBB with adsorbed BMP2, or DBB with BioCaP (Figure 7C). This finding indicated that BMP2-cop.BioCaP could not only induce bone formation efficiently but also significantly suppress the host foreign-body reaction to DBB. Such suppression was most probably attributed to the extensive osteogenesis.<sup>15</sup> The suppression of osteogenic activity on the formation of FBGCs may be partially mediated by the elevated levels of osteopontin, which is enriched during bone regeneration. Osteopontin was previously shown to suppress the fusion of macrophages into FBGCs both in vitro and in vivo.<sup>38</sup>

The volume ratio of FBGCs to DBB in the group of DBB with adsorbed BMP2 is similar with that in the group of DBB alone. This finding indicated that the transient high local concentration of BMP2 that was generated by its burst release did not influence the formation and accumulation of FBGCs at the 5-week juncture. Because bone-formation activity cannot be sustained when BMP2 was liberated in a single high-dose burst, the volume density of osseous tissue that was laid down was low (Figure 7A) and insufficient to hinder the formation of FBGCs (Figure 7C).

## CONCLUSIONS

In this study, we developed a novel BMP2-cop.BioCaP as an independent slow delivery system for BMP2. BMP2-cop.BioCaP can serve as “osteoiducer” to induce bone-formation efficiently and to suppress the foreign-body reaction to a clinically used bone-defect-filling material. In addition, this material also exhibited proper degradability. All these properties confer this BMP2-cop.BioCaP a very promising potential for the application clinically to repair large-size bone defects.

## DISCLOSURE

The authors have no conflicts of interest.

## ACKNOWLEDGMENT

We sincerely thank Prof. Dr. Tony Hearn for editing the grammar.

## REFERENCES

- Park JW, Jang JH, Bae SR, An CH, Suh JY. Bone formation with various bone graft substitutes in critical-sized rat calvarial defect. *Clin Oral Implants Res* 2009; 20:372–378.
- Sokolsky-Papkov M, Agashi K, Olaye A, Shakesheff K, Domb AJ. Polymer carriers for drug delivery in tissue engineering. *Adv Drug Deliv Rev* 2007; 59:187–206.
- Bannister SR, Powell CA. Foreign body reaction to anorganic bovine bone and autogenous bone with platelet-rich plasma in guided bone regeneration. *J Periodontol* 2008; 79:1116–1120.
- Liu Y, de Groot K, Hunziker EB. BMP-2 liberated from biomimetic implant coatings induces and sustains direct ossification in an ectopic rat model. *Bone* 2005; 36:745–757.
- Lou J, Xu F, Merkel K, Manske P. Gene therapy: adenovirus-mediated human bone morphogenetic protein-2 gene transfer induces mesenchymal progenitor cell proliferation and differentiation in vitro and bone formation in vivo. *J Orthop Res* 1999; 17:43–50.
- Govender S, Csimma C, Genant HK, et al. Recombinant human bone morphogenetic protein-2 for treatment of open tibial fractures: a prospective, controlled, randomized study of four hundred and fifty patients. *J Bone Joint Surg Am* 2002; 84-A:2123–2134.
- Zhao M, Zhao Z, Koh JT, Jin T, Franceschi RT. Combinatorial gene therapy for bone regeneration: cooperative interactions between adenovirus vectors expressing bone morphogenetic proteins 2, 4, and 7. *J Cell Biochem* 2005; 95:1–16.
- Schwarz F, Rothamel D, Herten M, et al. Lateral ridge augmentation using particulated or block bone substitutes biocoated with rhGDF-5 and rhBMP-2: an immunohistochemical study in dogs. *Clin Oral Implants Res* 2008; 19:642–652.
- Haidar ZS, Hamdy RC, Tabrizian M. Delivery of recombinant bone morphogenetic proteins for bone regeneration and repair. Part B: delivery systems for BMPs in orthopaedic and craniofacial tissue engineering. *Biotechnol Lett* 2009; 31:1825–1835.
- Haidar ZS, Hamdy RC, Tabrizian M. Delivery of recombinant bone morphogenetic proteins for bone regeneration and repair. Part A: current challenges in BMP delivery. *Biotechnol Lett* 2009; 31:1817–1824.
- Shields LB, Raque GH, Glassman SD, et al. Adverse effects associated with high-dose recombinant human bone morphogenetic protein-2 use in anterior cervical spine fusion. *Spine* 2006; 31:542–547.
- Smith DM, Cooper GM, Mooney MP, Marra KG, Losee JE. Bone morphogenetic protein 2 therapy for craniofacial surgery. *J Craniofac Surg* 2008; 19:1244–1259.
- Toth JM, Boden SD, Burkus JK, et al. Short-term osteoclastic activity induced by locally high concentrations of recombinant human bone morphogenetic protein-2 in a cancellous bone environment. *Spine (Phila Pa 1976)* 2009; 34:539–550.
- Wu G, Liu Y, Iizuka T, Hunziker EB. The effect of a slow mode of BMP-2 delivery on the inflammatory response provoked by bone-defect-filling polymeric scaffolds. *Biomaterials* 2010; 31:7485–7493.
- Wu G, Hunziker EB, Zheng Y, Wismeijer D, Liu Y. Functionalization of deproteinized bovine bone with a coating-incorporated depot of BMP-2 renders the material efficiently osteoinductive and suppresses foreign-body reactivity. *Bone* 2011; 49:1323–1330.
- Liu Y, Wu G, de Groot K. Biomimetic coatings for bone tissue engineering of critical-sized defects. *J R Soc Interface* 2010; 7 (Suppl 5):S631–S647.
- Liu Y, Hunziker EB, Layrolle P, De Bruijn JD, De Groot K. Bone morphogenetic protein 2 incorporated into biomimetic coatings retains its biological activity. *Tissue Eng* 2004; 10:101–108.
- Liu Y, Huse RO, de Groot K, Buser D, Hunziker EB. Delivery mode and efficacy of BMP-2 in association with implants. *J Dent Res* 2007; 86:84–89.
- De Lumen BO, Tappel AL. Fluorescein-hemoglobin as a substrate for cathepsin D and other proteases. *Anal Biochem* 1970; 36:22–29.
- Gundersen HJ, Jensen EB. The efficiency of systematic sampling in stereology and its prediction. *J Microsc* 1987; 147:229–263.
- Schenk RK, Olah AJ, Herrmann W. Preparation of calcified tissues for light microscopy. In: Ds GR, ed. *Proceedings of the methods of calcified tissue preparation*. New York: Elsevier Science Publishers B.V., 1984:1–56.
- Ballanti P, Minisola S, Pacitti MT, et al. Tartrate-resistant acid phosphate activity as osteoclastic marker: sensitivity of cytochemical assessment and serum assay in comparison with standardized osteoclast histomorphometry. *Osteoporos Int* 1997; 7:39–43.
- Cavalieri B. *Geometria Indivisibilibus Continuorum. Proceedings of the*, 1635. Reprinted as *Geometria degli Indivisibili*. Torino: Unione Tipografico-Editorice Torinese, 1966.
- Cruz-Orive LM, Weibel ER. Recent stereological methods for cell biology: a brief survey. *Am J Physiol* 1990; 258: L148–L156.
- Liu Y, Enggist L, Kuffer AF, Buser D, Hunziker EB. The influence of BMP-2 and its mode of delivery on the

- osteointegration. *Biomaterials* 2007; 28:2677–2686.
26. Wu G, Liu Y, Iizuka T, Hunziker EB. Biomimetic coating of organic polymers with a protein-functionalized layer of calcium phosphate: the surface properties of the carrier influence neither the coating characteristics nor the incorporation mechanism or release kinetics of the protein. *Tissue Eng Part C Methods* 2010; 16:1255–1265.
  27. Tanuma Y, Anada T, Honda Y, et al. Granule size-dependent bone regenerative capacity of octacalcium phosphate in collagen matrix. *Tissue Eng Part A* 2012; 18:546–557.
  28. Bose S, Tarafder S. Calcium phosphate ceramic systems in growth factor and drug delivery for bone tissue engineering: a review. *Acta Biomater* 2012; 8:1401–1421.
  29. Heymann D, Pradal G, Benahmed M. Cellular mechanisms of calcium phosphate ceramic degradation. *Histol Histopathol* 1999; 14:871–877.
  30. Anderson JM, Rodriguez A, Chang DT. Foreign body reaction to biomaterials. *Semin Immunol* 2008; 20:86–100.
  31. Blair HC, Schlesinger PH, Huang CL, Zaidi M. Calcium signalling and calcium transport in bone disease. *Subcell Biochem* 2007; 45:539–562.
  32. Kohn DH, Sarmadi M, Helman JJ, Krebsbach PH. Effects of pH on human bone marrow stromal cells in vitro: implications for tissue engineering of bone. *J Biomed Mater Res* 2002; 60:292–299.
  33. Nagano M, Nakamura T, Kokubo T, Tanahashi M, Ogawa M. Differences of bone bonding ability and degradation behaviour in vivo between amorphous calcium phosphate and highly crystalline hydroxyapatite coating. *Biomaterials* 1996; 17:1771–1777.
  34. Araujo MG, Lindhe J. Socket grafting with the use of autologous bone: an experimental study in the dog. *Clin Oral Implants Res* 2011; 22:9–13.
  35. Zambuzzi WF, Oliveira RC, Pereira FL, et al. Rat subcutaneous tissue response to macrogranular porous anorganic bovine bone graft. *Braz Dent J* 2006; 17:274–278.
  36. Ratner BD, Bryant SJ. Biomaterials: where we have been and where we are going. *Annu Rev Biomed Eng* 2004; 6:41–75.
  37. Salthouse TN. Some aspects of macrophage behavior at the implant interface. *J Biomed Mater Res* 1984; 18:395–401.
  38. Tsai AT, Rice J, Scatena M, et al. The role of osteopontin in foreign body giant cell formation. *Biomaterials* 2005; 26:5835–5843.

Copyright of Clinical Implant Dentistry & Related Research is the property of Wiley-Blackwell and its content may not be copied or emailed to multiple sites or posted to a listserv without the copyright holder's express written permission. However, users may print, download, or email articles for individual use.